2-1-2005

Resonant light interaction with plasmonic nanowire systems

Viktor Podolskiy
Oregon State University

Andrey Sarychev
Ethertronics Incorporated

Evgenii Narimanov
Purdue University, evgenii@purdue.edu

Vladimir Shalaev
Purdue University, shalaev@purdue.edu

INSTITUTE OF PHYSICS PUBLISHING JOURNAL OF OPTICS A: PURE AND APPLIED OPTICS

J. Opt. A: Pure Appl. Opt. **7** (2005) S32–S37 doi:10.1088/1464-4258/7/2/004

Resonant light interaction with plasmonic nanowire systems

Viktor A Podolskiy[1,2,5], Andrey K Sarychev[3], Evgenii E Narimanov[2] and Vladimir M Shalaev[4]

[1] Physics Department, Oregon State University, Corvallis, OR 97331, USA
[2] Electrical Engineering Department, Princeton University, Princeton, NJ 08540, USA
[3] Ethertronics Incorporated, 9605 Scranton Road, Suite 850, San Diego, CA 92121, USA
[4] School of Electrical and Computer Engineering, Purdue University, West Lafayette, IN 47907, USA

E-mail: vpodolsk@physics.orst.edu

Received 3 June 2004, accepted for publication 6 October 2004
Published 20 January 2005
Online at stacks.iop.org/JOptA/7/S32

Abstract
We compare the optical response of isolated nanowires, double-wire systems, and Π-structures, and show that their radiation is well described in terms of their electric and magnetic dipole moments. We also show that both dielectric permittivity and magnetic permeability can be negative at optical and near infrared frequencies, and demonstrate the connection between the geometry of the system and its resonance characteristics. We conclude that plasmonic nanowires can be employed for novel negative-index materials. Finally, we demonstrate that it is possible to construct a nanowire-based 'transparent nanoresonator' with dramatically enhanced intensity and metal concentration below 5%.

Keywords: left-handed media, resonance, nanomaterials, nanowires

1. Introduction

The concept of light manipulation on the subwavelength scale is increasingly attractive to researchers in optics, materials science, and chemistry [1–3]. Plasmonic materials, strongly interacting with light, are the exceptional candidates for the nanophotonic devices. It has been shown that the metallic nanoparticles can effectively confine the optical radiation to 'nanoscale' in the proximity of plasmon resonance; the shape and position of this resonance is controlled by the shape of the nanoparticles (or their clusters) [4–11]. The broadband confinement can be achieved in metal-dielectric films [1, 12, 13]. Also, the resonant nanoelements can be employed to transmit the optical light at nanoscales [14, 15]. Another class of nanoplasmonic devices based on metallic nanowires and nanowire pairs has been suggested to obtain light nanoconfinement, transmission, and even negative refraction for optical and infrared frequencies [16, 17] due to resonance excitation of electric and magnetic dipole moments. However, while the dipole contribution dominates the forward and backward scattering of the nanowire systems, the presence of quadrupole moment may substantially affect their 'side' scattering characteristics.

Here we address the electromagnetic response of the nanowire systems, and show that it is indeed dominated by the dipole moments. We also demonstrate that the electric and magnetic resonances correspond to a special kind of surface (plasmon polariton) wave, and can be independently controlled using the combination of nanowires and Π-structures [18]. Finally, we show that the nanowire composites may be used to build a 'broadband transparent nanoresonator', achieving an *average* intensity enhancement exceeding an order of magnitude, with a metal concentration less than 5%. The rest of the paper is organized as follows. We first briefly describe the typical nanowire geometry and the coupled dipole equations (CDEs) used in our simulations. We then describe the resonant response of a single nanowire, nanowire pair and Π-structures. Finally, we demonstrate the field enhancement in the *transparent* nanowire composite.

[5] Author to whom any correspondence should be addressed.

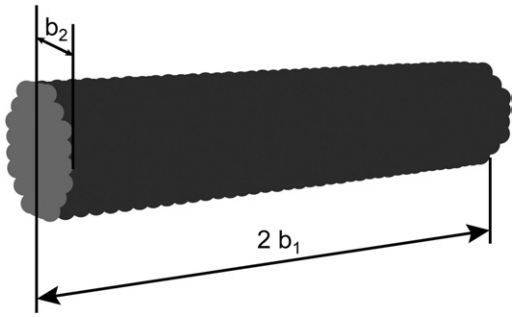

Figure 1. A long nanowire represented by an array of point dipoles.

2. Simulation of the nanowire response using CDEs

The typical radius of individual nanowires described in this paper, b_2, is much smaller than the wavelength of the incident light, λ, and is comparable with the skin-depth of the material. The length of the wire, $2b_1$, on the other hand, is comparable to the wavelength (see figure 1). The electromagnetic properties of such metallic nanostructures are somewhat similar to the properties of scaled-down radio-antennas widely used in telecommunications. However, the finite value of the dielectric constant of the metal in the optical range and typically low aspect ratio lead to the fundamental differences in the response of optical- and radio-antennas. These differences make the analytical solution for the problem of electromagnetic response of nanowires hardly possible. To find the response of our system we use the well-known coupled-dipole approximation [17, 19, 20].

In this approach, the system is represented by an array of point dipoles arranged at the sites of a cubic lattice. Each dipole is subjected to the field of an incident plane wave and to the field of all other dipoles. Thus, the dipole moments of all dipoles are coupled through the following *coupled-dipole equations* (CDEs):

$$\mathbf{d}_i = \alpha_0 \left[\mathbf{E}_{\text{inc}} + \sum_{j \neq i}^{N} \hat{G}(\mathbf{r}_i - \mathbf{r}_j)\mathbf{d}_j \right], \tag{1}$$

where E_{inc} represents the incident field at the location of the ith dipole, $\mathbf{r}_i$, $\hat{G}(\mathbf{r}_i - \mathbf{r}_j)\mathbf{d}_j$ represents the EM field scattered by the dipole j at this point, and $\hat{G}$ is a regular part of the free-space dyadic Green function defined as

$$\begin{aligned} G_{\alpha\beta} &= k^3[A(kr)\delta_{\alpha\beta} + B(kr)r_\alpha r_\beta], \\ A(x) &= [x^{-1} + \mathrm{i}x^{-2} - x^{-3}]\exp(\mathrm{i}x), \\ B(x) &= [-x^{-1} - 3\mathrm{i}x^{-2} + 3x^{-3}]\exp(\mathrm{i}x), \end{aligned} \tag{2}$$

with $\hat{G}\mathbf{d} = G_{\alpha\beta}d_\beta$. The Greek indices represent the Cartesian components of vectors, and the summation over the repeated indices is implied.

The key parameter in CDEs is the polarizability of a monomer, α_0, usually given by Clausius–Mossotti relation (see, e.g. [21]) with the radiative correction introduced by Draine [20] (see also footnote below[6]):

$$\alpha_{\text{LL}} = R^3 \frac{\epsilon - 1}{\epsilon + 2}, \tag{3}$$

$$\alpha_0 = \frac{\alpha_{\text{LL}}}{1 - \mathrm{i}(2k^3/3)\alpha_{\text{LL}}}, \tag{4}$$

where ϵ is the dielectric permittivity of the material and α_{LL} is the Lorentz–Lorenz polarizability without the radiation correction. The magnitude of this polarizability, controlled by the parameter R, serves as a fitting parameter. It may be visualized as the radius of an imaginary sphere centred over the position of a point dipole. In our simulations this parameter is determined by the condition that the system response in the quasi-static limit yields the correct depolarization factors, and typically varies in the range $R = 0.59$–0.62 (in units of the lattice size).

In our numerical simulations we assume that the system composed from isolated (or coupled) silver nanowires is suspended in vacuum and excited with plane electromagnetic wave. We neglect the possible interference from dielectric substrates since

(i) it strongly depends on the materials properties of such substrate; and
(ii) it does not change the fundamental resonant effects presented here.

To describe the frequency-dependent dielectric constant of silver, $\epsilon_m(\omega)$, we use the well-known Drude model [23]: $\epsilon_m = \epsilon_\infty + \omega_{\text{p}}^2/(\omega^2 + \mathrm{i}\tau\omega)$ with plasma frequency $\omega_{\text{p}} = 9.1$ eV, damping constant $\tau = 0.021$ eV, and (non-resonant) interband-transition contribution $\epsilon_\infty = 5$. The possible discrepancy between the exact and model values of $\epsilon_m(\omega)$ due to material composition, finite size or temperature effects, resonant interband transitions, etc will not affect the existence of the resonant phenomena described below, and will only result in a quantitative shift between the positions of the resonances in actual experiments and the numerical results presented here.

The solution of the CDEs (in our simulations we use the direct matrix inversion) provides us with complete information about the system response. Thus, the electric and magnetic dipole moments directly follow from the CDE solutions; the electromagnetic field at any given point can be found by adding the incident field and the field scattered by all point dipoles.

3. Radiation and resonance properties of metallic nanowires

The non-resonant scattering by a nanostructured system typically weakly affects the incident electromagnetic radiation, and can be effectively treated by a variety of mostly perturbative techniques (see, e.g. [21]). However, when the frequency of incident light coincides with the resonant frequency of a nanostructure, the electromagnetic field distribution may be dominated by the scattered (radiated), and not the incident, wave. The wave scattered by a nanostructure can be expanded into the series of multipole components. The first term in such an expansion corresponds to the electric dipole component. The next two terms correspond to the magnetic dipole and the electric quadrupole [17, 21].

Similarly to the well-known case of radio-antennas [21], the radiation properties of an isolated nanowire are well

[6] It has been shown that the results of CDA weakly depend on the type of radiation correction [22] provided that $a\sqrt{\epsilon}/\lambda \ll 1$. In our calculations $a\sqrt{\epsilon}/\lambda \approx 1/10$.

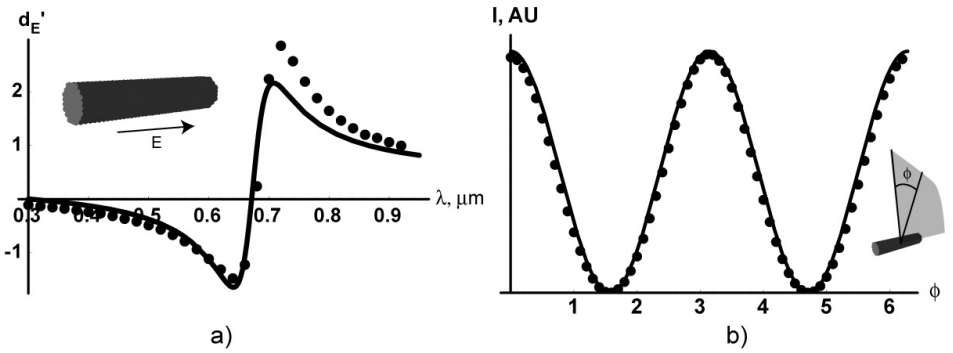

Figure 2. (a) The comparison between the dipole moment found from numerical simulations as described in section 2 (dots) and calculated using equation (5) (curve). The moments are normalized by unit volume. (b) The far-field intensity radiation pattern of a single nanowire in (a) is obtained from numerical simulations (dots) and calculated by approximating the antenna by a point dipole (solid curve) as a function of the angle ϕ (in radians) between the direction of scattering and the normal to the vector of the dipole moment (the nanowire axis). The dimensions of the silver wire are 162 nm × 32 nm × 32 nm. The far-field pattern is calculated for $\lambda = 560$ nm. The E-field is parallel to the nanowire ((a), inset).

described by its dipole moment alone. This fact is illustrated in figure 2(b), where we calculate the intensity of the scattered field by the single silver nanowire as a function of the angle ϕ between the normal to the nanowire and the scattering direction.

The induced polarization in a substantially long and thin wire ($b_2 \ll b_1; b_2 \ll \lambda$) close to its first resonance ($2b_1 = \lambda_p/2$, where λ_p is the wavelength of the plasmon polariton) can be represented by the following relation [24]) (see figure 2(a)):

$$d_E = \tfrac{2}{3}\left[b_1 b_2^2 f(\Delta) E \epsilon_m\right] \times \left[1 + f(\Delta)\epsilon_m \frac{b_1^2}{b_2^2} \ln\left(1 + \frac{b_1}{b_2}\right)\cos\Omega\right]^{-1}, \quad (5)$$

where the dimensionless frequency Ω is given by $\Omega^2 = (b_1 k)^2 \frac{\ln(b_1/b_2) + ikb_1}{\ln(1+b_1/b_2)}$. The function $f(\Delta) = \frac{1-i}{\Delta}\frac{J_1[(1+i)\Delta]}{J_0[(1+i)\Delta]}$ accounts for the skin effect; the parameter $\Delta = b_2\sqrt{2\pi\sigma_m\omega/c}$ represents the ratio of the nanowire radius to the skin depth, σ_m is the bulk metal conductivity, $k = 2\pi/\lambda$ is the free-space wavevector, $\omega = 2\pi c/\lambda$ is the frequency of the incident radiation, and c is the speed of light in vacuum.

The resonances in an isolated nanowire (figure 2) can be related to the resonant excitations of a special kind of surface wave on the metal–air interface. These waves, which exponentially decay away from the interface, are also known as plasmon polaritons. Although the excitation of the plasmon polariton with a plane electromagnetic wave is impossible in the infinite medium (see e.g. [25]), the plasmon waves have non-zero resonance width in *finite* nanowires so they can effectively couple to a plane wave. The frequency of the polariton resonance is controlled by the nanowire material and length, while the 'width' of this resonance is related to the skin-depth and the radius of the wire [17]. This effect makes it possible to use a single metallic nanoantenna to confine and transmit the optical and infrared radiation *on the nanoscale* [16, 17].

The behaviour of the plasmon modes changes substantially when two nanowires are positioned closely to each other, so that their centres are separated by the distance $d \ll \lambda$ and their plasmon modes can interact with each other. When the electric field of the incident plane wave is parallel to the wires, and the magnetic field is perpendicular to the common plane of the two wires (see figure 3), two kinds of plasmon polariton waves of the different symmetry can be excited.

The symmetric combination of the two polariton waves leads to the excitation of the dipole moment in both wires. In this case, the electric field of the incident plane wave resonantly excites parallel currents in both nanowires. The anti-symmetric combination, on the other hand, corresponds to the *anti-parallel currents* in the two wires (excited by a magnetic field component of the incident wave). These currents, together with the displacement currents in between the wires, lead to a resonant excitation of the *magnetic dipole moment* in the system. The shift between the resonance frequencies of the electric and magnetic dipoles is related to a coupling efficiency between the polariton modes in the two wires, which in turn is controlled by the distance between the wires. This effect has a similar nature to the splitting of the energy levels of the wavefunctions of different symmetry in the double-well potential due to the tunnelling coupling.

The effect of the polariton modes' interaction on the resonance characteristics is clearly seen when we compare the electric and magnetic response of the system of two parallel nanowires and of the Π-system of the same size, which is obtained by bringing one end of the two wires into the electric contact (see figure 3(d)). As is explained above, the electric resonant response of the system is governed by the symmetric polariton mode. The currents in the two nanowires in this case have essentially the same distribution, so they are not affected by the electric contact between wires. The magnetic response of the two systems, on the other hand, is dramatically different, since the presence of the electric contact forces the connected points to have the same value of the potential, and this makes the excitation of the anti-symmetric polariton mode impossible.

Due to the presence of the electric contact, the magnetic resonances of the Π-structure do not directly correspond to the electric resonances of the single nanowire. It can be shown that the Π-structure may have a resonant magnetic response even when its size is much smaller than the wavelength, so that no polariton modes can propagate on the corresponding nanowire. The magnetic resonance in this case is similar to the electric plasmon resonance which occurs in all metallic nanoparticles. In the limit of $\lambda \gg b_1 \gg d \gg b_2$ the magnetic

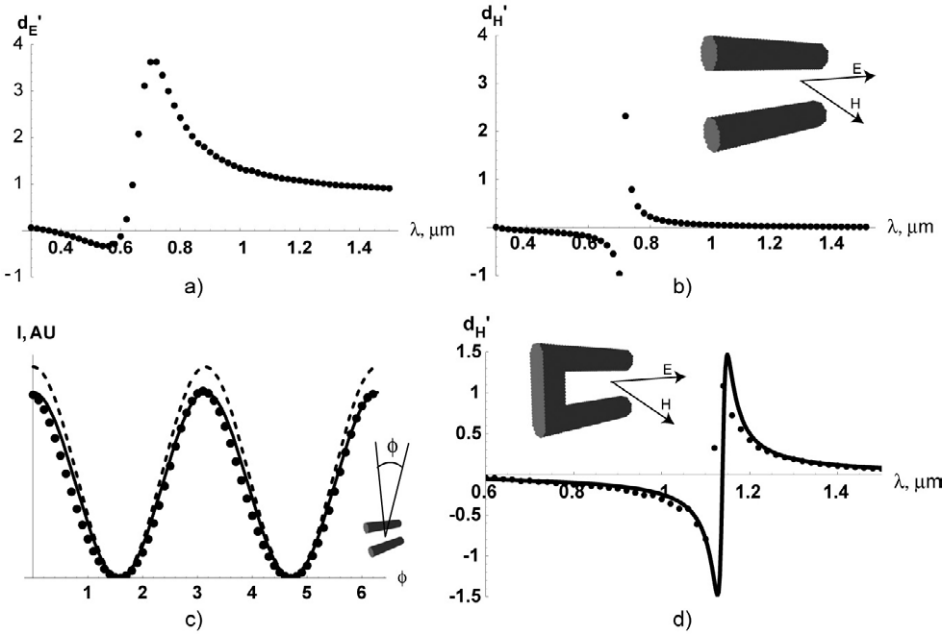

Figure 3. (a) The dipole moment of the coupled nanowire system with dimensions 162 nm (antenna length) by 32 nm (antenna diameter) by 80 nm (distance between antennas). (b) The magnetic dipole moment of the system in (a). (c) The far-field intensity distribution of the system in (a) and (b) as a function of the angle ϕ (in radians) between the direction of scattering and the normal to the vector of the dipole moment (the nanowire axis) ((c), inset), calculated using CDE simulations as described in the text (dots), by approximating the system by a point electric dipole (dashed curve) and by approximating the system by point electric and magnetic dipoles (solid curve). The far-field pattern is calculated for $\lambda = 560$ nm. (d) Connecting the coupled nanowires in (a) and (b) into a Π-structure drastically shifts the position of the magnetic resonance, leaving the dipole moment of the system practically unchanged (not shown). The dots correspond to numerical simulations, and the solid curve corresponds to equation (6). All moments are normalized by the unit volume. The E-field is parallel to the nanowire; the H-field is perpendicular to the nanowire plane ((b), inset).

resonance of the Π-structure can be described by the following expression [18]:

$$d_H = \frac{1}{2} H_0 b_1^3 \log(d/b_1)(kd)^2 \frac{\tan(gb_1) - gb_1}{(gb_1)^3}, \qquad (6)$$

where $g^2 \approx -4\log(d/b_2)/(b_2^2/\epsilon)$. Note that the frequency of this *magnetic plasmon resonance* is defined solely by the geometry of the system and not by the wavelength, similarly to the well-known case of (dipole) plasmon resonance.

As a result of the two-wire interaction, the scattering (far-field) response of the coupled wire systems and Π-structures, which defines the interaction between different elements in the macroscopic composite, is not described by the dipole moment alone. As is shown in figures 3(a) and (b), such systems have magnetic dipole moments comparable to their electric dipole moments. Our numerical simulations clearly show that these systems are fully described by two dipole moments, and have vanishing higher moments. This in turn leads to highly-directional emission (scattering) properties of the double-wire systems. This fact is illustrated in figure 3(c), which shows excellent agreement between the far field obtained by numerical calculation and by approximating the system by point electric and magnetic dipoles.

As described in section 4, the electric and magnetic resonances can be used to produce extremely high local fields, which may be beneficial for a variety of spectroscopic, lithographic, and biological applications.

In particular, one of the most promising applications of nanowire composites lies in the area of materials with simultaneously negative dielectric permittivity and magnetic permeability. Such media, originally considered by Veselago [26], were predicted to have a negative refractive index and consequently exhibit a wide variety of surprising optical phenomena. Among them are the reversed Snell's law [27–31], Cherenkov radiation, and Doppler effect [27–31]. Due to their negative phase velocity such media are often referred to as 'left-handed', meaning that the wavevector and the vectors of electric and magnetic fields form in such a material a left-handed trio in contrast to the conventional 'right-handed' case. One of the most promising phenomena present in left-handed materials is so-called 'superlensing', where a slab of a medium with $\epsilon = \mu = -1$ is used to obtain an optically perfect image with subwavelength resolution in the far field [32–35].

As we showed above, the system of coupled nanoantennas exhibits a resonance electric and magnetic response. When the wavelength of an incident light is below the resonance in the coupled nanowire system, the excited moments are directed opposite to the excitation field (figure 3). Such negative responses may be used to implement a left-handed composite in the optical and near-infrared ranges [16–18, 36].

By changing the geometry of the system we can shift the resonances to any region from the visible to near infrared frequency ranges [16, 17, 36].

4. Enhanced local fields in nanoantenna arrays

As was mentioned above, the resonance coupling between the plane and polariton waves in a single metallic nanowire opens

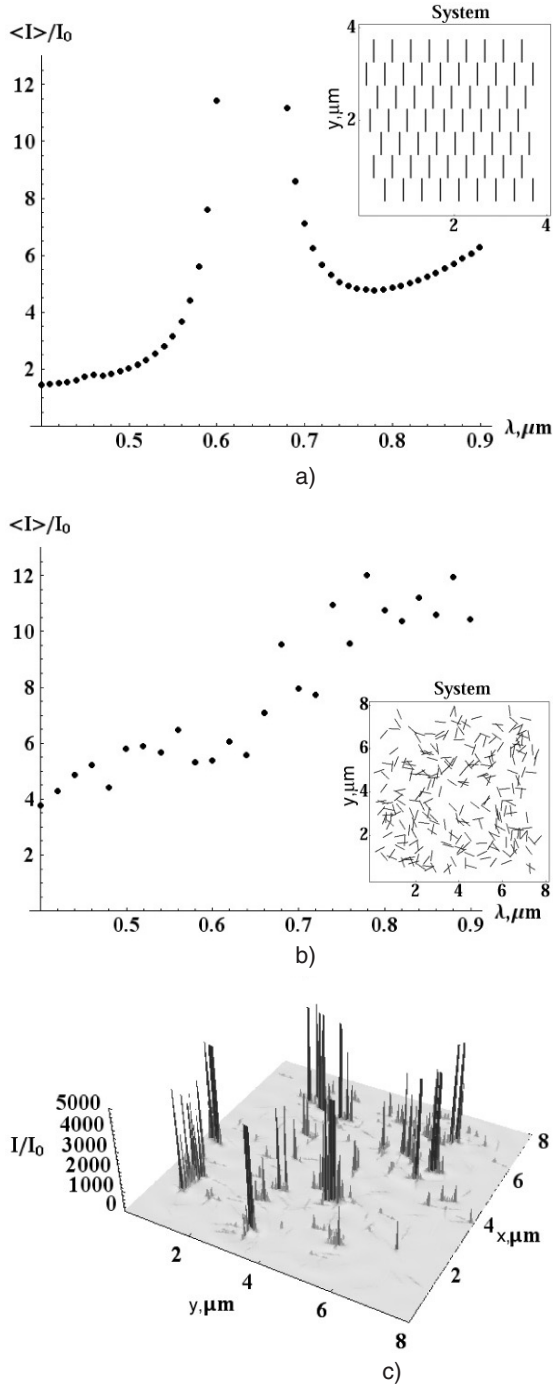

Figure 4. (a) The average near-field intensity $\langle I \rangle$ over the parallel wire composite (inset) clearly shows a separated-resonance structure, an implicit property of a single nanowire. (b) The random nanowire percolation composite (inset) exhibits a broadband intensity enhancement due to collective excitation of a large number of different resonant clusters. The intensity distribution over this composite for $\lambda = 800$ nm is shown in (c). The size of the individual wire in both composites is 600 nm $\times$ 20 nm $\times$ 20 nm; the surface concentration of metal is 4%; normal incidence with $E \parallel y$ is used; the intensity is calculated at a height 24 nm from the composite; the average intensity is normalized to the intensity of the incident field.

a possibility to propagate the optical light through the array of nanoantennas, using them as wires in all-optical computers and telecommunication systems. It also opens the possibility of resonant light amplification on the nanoscale due to the resonant excitation of polariton waves.

The local intensity in this case can exceed the intensity of the incident field by three or more orders of magnitude (figure 4). Such high local fields are beneficial for enhanced spectroscopy, lithography, absorption, nonlinear processes and all related applications. Note that high local fields at the resonance are usually accompanied by the narrow frequency band where the resonance exists [17]. The resonant frequency itself is controlled by the length of the nanowire and its material.

While the area of the enhanced local field is concentrated near the nanoantenna surface, the collective resonance of several antennas can lead to the enhancement of the *average* intensity in the antenna composite. The response of the equally separated parallel nanowires resembles the behaviour of an isolated antenna (figure 4(a)), exhibiting huge intensity enhancement in the narrow frequency ranges corresponding to the 'eigen' frequencies of the plasmon polariton waves in the individual wires.

The situation changes dramatically when the antennas are randomly deposited on a dielectric substrate, and a surface metal concentration reaches the value when the composite starts to conduct a DC current (known as the percolation threshold). At this point the composite contains nanowire clusters of all possible sizes and configurations, each having its own resonance frequency, and generating at this frequency high local fields. The collective effect of all the clusters leads to the extremely broadband intensity enhancement, as shown in figure 4(b). This effect is similar to the broadband field excitation in a conventional percolation film [1, 12]. However, in contrast to the percolation film, where the percolation threshold concentration is fixed and is equal to 50%, the percolation threshold in a nanowire composite is inversely proportional to the aspect ratio of the individual nanowires and can be made arbitrarily small, making it possible to fabricate a 'transparent nanoresonator'. This system can be effectively used in the areas which require simultaneously high fields and optical transparency, e.g. in stacked solar cells [37], transparent bio-sensors or optical lithography.

5. Conclusion

The unique resonant characteristics of metallic nanoantennas could be precisely controlled by their geometry and material properties. The polariton resonance frequency in such devices can be tuned to any given range from the optical to the mid-infrared. Applications of plasmonic nanowire composites include narrow- and broadband nanoresonators, photonics, and left-handed media.

Acknowledgments

This work was supported in part by NSF under ECS-0210445, ECS-0400615, DMR-0134736, and DMR-0121814 grants.

References

[1] Shalaev V M (ed) 2002 *Optical Properties of Random Media* (Berlin: Springer)

[2] Bertolotti M, Bowden C M and Sibilia C (ed) 2001 *Nanoscale Linear and Nonlinear Optics* (*AIP Conf. Proc. Series* vol 560) (New York: American Institute of Physics) and references therein
[3] Brown S D M, Corio P, Marucci A, Pimenta M A, Dresselhaus M S and Dresselhaus G 2000 *Phys. Rev.* B **61** 7734
Shelimov K B and Moskovits M 2000 *Chem. Mater.* **12** 250
Li J, Papadopoulos C, Xu J M and Moskovits M 1999 *Appl. Phys. Lett.* **75** 367
[4] Jin R, Cao Y, Mirkin C A, Kelly K L, Schatz G C and Zheng J 2001 Photo induced conversion of silver nanospheres to nanoprisms *Science* **294** 1901
[5] Haynes C L, McFarland A D, Zhao L and Van Duyne R P 2003 Nanoparticle optics: the importance of radiative dipole coupling in two-dimensional nanoparticle arrays *J. Phys. Chem.* B **107** 7337
[6] Zhao L, Kelly K L and Schatz G C 2003 The extinction spectra of silver nanoparticle arrays: influence of array structure on plasmon resonance wavelength and width *J. Phys. Chem.* B **107** 7343
[7] Pipino A C R, Schatz G C and Van Duyne R P 1994 Surface-enhanced second-harmonic diffraction: selective enhancement by spatial harmonics *Phys. Rev.* B **49** 8320
[8] Jin R *et al* 2003 Controlling anisotropic nanoparticle growth through plasmon excitation *Nature* **425** 487
[9] Murphy C J, Jana N R, Gearheart L A, Obare S O, Caswell K K, Mann S, Johnson C J, Davis S A, Dujardin E and Edler K 2004 Synthesis, assembly and reactivity of metallic nanorods *Chemistry of Nanomaterials* ed C N R Rao, A Muller and A Cheetham (Weinheim: Wiley–VCH)
[10] Caswell K K, Bender C M and Murphy C J 2003 Seedless, surfactantless wet chemical synthesis of silver nanowires *Nano Lett.* **3** 667
[11] Charnay C *et al* 2003 Reduced symmetry metallodielectric nanoparticles: chemical synthesis and plasmonic properties *J. Phys. Chem.* B **107** 7327
[12] Ducourtieux S *et al* 2001 *Phys. Rev.* B **64** 165403
[13] Haynes C L and van Duyne R P 2003 Sampled surface-enhanced Raman excitation spectroscopy *J. Phys. Chem.* B **107** 7426
[14] Sarychev A K, Podolskiy V A, Dykhe A M and Shalaev V M 2002 *IEEE J. Quantum Electron.* **38** 956
[15] Maier S A *et al* 2003 Local detection of electromagnetic energy transport below the diffraction limit in metal nanoparticle plasmon waveguides *Nat. Mater.* **2** 229
[16] Podolskiy V A, Sarychev A K and Shalaev V M 2002 *J. Nonlinear Opt. Phys. Mater.* **11** 65
[17] Podolskiy V, Sarychev A and Shalaev V 2003 *Opt. Express* **11** 735
[18] Sarychev A K and Shalaev V M 2004 *Magnetic Resonance in Metal Nanoantennae, SPIE Proc.* **5508** 128–37
[19] Purcell E M and Pennypacker C R 1973 *Astrophys. J.* **405** 705
[20] Draine B T 1988 *Astrophys. J.* **333** 848
[21] Jackson J D 1999 *Classical Electrodynamics* (New York: Wiley)
[22] Draine B T and Goodman J 1993 Beyond Clausius Mossotti: wave propagation on a polarizable point lattice and the discrete dipole approximation *Astrophys. J.* **405** 685
Draine B T and Flatau P J 1994 Discrete-dipole approximation for scattering calculations *J. Opt. Soc. Am.* A **11** 1491
[23] Kittel 1976 *Introduction to Solid State Physics* (New York: Wiley)
[24] Lagarkov A N and Sarychev A K 1996 *Phys. Rev.* B **53** 10
Maknovskiy D P, Panina L V, Mapps D J and Sarychev A K 2001 *Phys. Rev.* B **64** 165403
[25] Landau L D, Lifshitz E M and Pitaevskii L P 2000 *Electrodynamics of Continuous Media* 2nd edn (Oxford: Pergamon)
[26] Veselago V G 1968 *Sov. Phys.—Usp.* **10** 509
[27] Cubukcu E, Aydin K, Ozbay E, Foteinopoulou S and Soukoulis C M 2003 *Nature* **423** 604
[28] Smith D R, Padilla W J, Vier D C, Nemat-Nasser S C and Shultz S 2000 *Phys. Rev. Lett.* **84** 4184
[29] Parazzoli C *et al* 2003 *Phys. Rev. Lett.* **90** 107401
[30] Shvets G 2003 *Phys. Rev.* B **67** 035109
[31] Iyer A K, Kremer P C and Eleftheriades G V 2003 *Opt. Express* **11** 696
[32] Pendry J B 2000 Negative refraction makes a perfect lens *Phys. Rev. Lett.* **85** 3966 see also [33]
[33] Podolskiy V A and Narimanov E E 2004 *Opt. Lett.* at press (*Preprint* physics/0403139)
Merlin R 2004 *Appl. Phys. Lett.* **84** 1290
Smith D R *et al* 2003 *Appl. Phys. Lett.* **82** 1506
[34] Cubukcu E, Aydin K, Ozbay E, Foteinopolou S and Soukoulis C M 2003 *Phys. Rev. Lett.* **91** 20
[35] Parimi P V, Lu W T, Vodo P and Sridhar S 2003 *Nature* **426** 404
[36] Sarychev A K, Drachev V P, Yuan H-K, Podolskiy V A and Shalaev V M 2003 *Optical Properties of Metal Nanowires, SPIE Proc.* **5219** 13
[37] Peumans P, Yakimov A and Forrest S R 2003 *J. Appl. Phys.* **93** 3693